Received: 29 July 2021 | Revised: 20 October 2021 | Accepted: 19 November 2021

DOI: 10.1002/hyp.14437

RESEARCH ARTICLE

WILEY

Snow drought reduces water transit times in headwater streams

Catalina Segura

Department of Forest Engineering, Resources and Management, College of Forestry, Oregon State University, Corvallis, Oregon, USA

Correspondence
Catalina Segura, Department of Forest Engineering, Resources, and Management, College of Forestry, Oregon State University, Corvallis, OR, USA.
Email: segurac@oregonstate.edu

Funding information
National Science Foundation, Grant/Award Numbers: 1943574, LTER7 DEB-1440409, LTER8 DEB-2025755; USDA National Institute of Food and Agriculture, Grant/Award Number: McIntire Stennis Project OREZ-FERM-876

Abstract

Knowledge of water transit times through watersheds is fundamental to understand hydrological and biogeochemical processes. However, its prediction is still elusive, particularly in mountainous terrain where physiography and precipitation change over short distances. In addition, much remains to be studied about the impact of climate change on transit time as it continues to change precipitation form in mountainous terrain. Water isotopic ratios were used to evaluate mean transit time (MTT) and young water fractions (F^*_{yw}) in seven small mountainous watersheds in western Oregon over the 2014–2018 period that included a major regional snow drought in 2015. The MTT was shorter in 2015 across all watersheds compared to any other year while the F^*_{yw} was larger in 2015 than in any other year. The short transit times observed in 2015 could be related to low connectivity between surface water and older ground water which resulted in a homogenous hydrologic response across all the investigated watersheds despite their physiographical differences. The 2016–2018 MTT vary widely across all watersheds but especially within the smaller high elevation watersheds indicating that the impact of the 2015 snow drought was stronger for systems that depend heavily on snowmelt inputs. During relatively wet/cold years intrinsic watershed characteristics such as drainage area and terrain roughness explained some of the variability in transit time metrics across all watersheds. Shorter transit times during the drought have implications for water quality and solute concentrations as biogeochemical processes are controlled in part by the time water resides and interacts within the subsurface. Although the impact of the 2015 snow drought appears short-lived these results are particularly critical considering the expected regional snowpack decline as the climate warms in the western United States.

KEYWORDS
climate change, gamma function, H.J. Andrews Experimental Forest, isotopes, mean transit time, Oregon, young water fraction

1 | INTRODUCTION

Understanding the physics that drives the hydrologic response of a watershed to precipitation is fundamental to predict water supply and the linkage between water movement and biogeochemical cycles. While the prediction of total discharge is often possible, the prediction of the relative time source (or age) of the water exiting a watershed is more complicated. Water age depends on factors that control the amount and form of the water input and the movement, mixing, and storage of water in the landscape. The understanding of these

processes is particularly crucial for headwater streams because water quantity and quality of freshwater systems depend on inputs from these smaller streams (Lowe & Likens, 2005). In these systems, many located in mountainous terrain, the prediction of water movement is complex because water storage capacity and overall water input magnitude and form vary over short distances given variable physiography (geology, geomorphology, and topography) and water inputs (rain versus snow). Furthermore, understanding patterns of water storage and release to downstream locations is critical because the hydrologic regime in many headwater streams is expected to change under projected declines in snowpack (Mote et al., 2018; Verfaillie et al., 2018). In the Pacific Northwest watersheds are particularly vulnerable to the impacts of climate because they depend on both winter rain and spring snowmelt (Vano et al., 2015).

Tracers such as water stable isotope ratios have been extensively used to estimate the travel time of water in terms of transit time distributions which reflect characteristic information about flow paths, storage, and sources of water (McGuire & McDonnell, 2006). The mean transit time (MTT) has been inferred in a variety of environments using lumped convolution modelling approaches (e.g., Bansah & Ali, 2019; Heidbuechel et al., 2012; Hrachowitz et al., 2010; McGuire et al., 2005; Mosquera et al., 2016; Soulsby & Tetzlaff, 2008). These approaches assume steady state conditions which have been shown to suffer from aggregation biases (Kirchner, 2016a; Kirchner, 2016b) especially when capturing short term features of the hydrologic response (Botter et al., 2010). Alternative time-variant approaches based on high resolution data have been proposed (e.g., Benettin et al., 2015; Benettin et al., 2017; Botter et al., 2011; Harman, 2015). Although the computational cost (Seeger & Weiler, 2014) of these approaches has become more manageable, the detailed tracer data required (Harman, 2015; Heidbuechel et al., 2012) remains a considerable constrain. Thus, although significant debate exists about the bias associated with the steady state condition assumption of the lumped convolution approach, it remains the most feasible alternative for studies with relatively sparse data (weekly–monthly sampling campaigns) which focus on the understanding of hydrologic processes rather than on the advancement of transit time modelling methods (Seeger & Weiler, 2014; Bansah & Ali, 2019).

Regardless of the method, transit time models are ultimately intended to describe water storage and release dynamics. As such many previous efforts have been focused on finding relationships between MTT and spatial intrinsic watershed characteristics such as topographic metrics (Hrachowitz et al., 2009; McGuire et al., 2005; Mosquera et al., 2016; Mueller et al., 2013; Tetzlaff et al., 2009), geology (Gabrielli & McDonnell, 2020; Hale & McDonnell, 2016), and soils characteristics (Capell et al., 2012; Soulsby & Tetzlaff, 2008). However, the results are site specific, preventing wide generalizations. For example, contrasting results have been found about terrain slope as a MTT controlling factor with some reporting strong correlations between MTT and slope or slope derivates (e.g., Leach et al., 2020; McGuire et al., 2005; Mosquera et al., 2016; Soulsby et al., 2006) and some reporting weak correlations (e.g., Seeger & Weiler, 2014; Hale & McDonnell, 2016; Bansah & Ali, 2019). Furthermore, studies have illustrated dynamic temporal variability in MTT within sites, depending on variations of precipitation input (Heidbuchel et al., 2013; Hrachowitz et al., 2009; Seeger & Weiler, 2014).

The young water fraction was recently introduced as a transit time metric that is not subject to aggregation bias (Kirchner, 2016a; Kirchner, 2016b). The young water fraction represents the proportion of a watershed outflow that is on average less than 2–3 months old. This metric has been used in a variety of environments, for example, boreal landscapes (Jutebring Sterte et al., 2021), karst environments (Simon et al., 2019; Zhang et al., 2020), and tropical watersheds (Trinh et al., 2020). In mountainous regions several studies have been conducted in European watersheds (Ceperley et al., 2020; Garvelmann et al., 2017; Stockinger et al., 2019) and North America (Campbell et al., 2020; Zhang et al., 2018). Like in the case of MTT, landscape features such as terrain slope derivates (Jasechko et al., 2016; von Freyberg et al., 2018) and bedrock ground water (Garvelmann et al., 2017), appear to control some of the observed variability in young water fraction. Discharge variability (Lutz et al., 2018; von Freyberg et al., 2018) and precipitation amount and form (Campbell et al., 2020; Ceperley et al., 2020; Stockinger et al., 2019; Zhang et al., 2018) also have explained young water fraction variability.

The objective of this article was to investigate the influence of the 2015 snow drought in the temporal and spatial variability of transit times across seven small headwater mountainous watersheds. Water isotope ratios collected between 2014 and 2018 were used as tracers to estimate mean transit times with the convolution approach as well as annual young water fractions. The results illustrate that the conditions during the 2015 snow drought resulted in faster mean transit times and larger young water fraction contributions than any other year.

2 | MATERIALS AND METHODS

2.1 | Study area

This study analyses the effects of the 2015 snow drought in runoff generation at seven nested watersheds in the Andrews Forest in the Western Cascade Range of Oregon (Figure 1). Mean elevation in the watersheds varies between 707 and 1195 m draining 21.4–6400 ha (Figure 1, Table 1). From high to low elevation: WS 07 and WS 08 drain into McRae Creek (MR), while Mack Creek (MACK) and WS 02 drain into Lookout Creek (LOOK), WS 01 also drains into LOOK downstream of the LOOK grab sampling site (Figure 1). The geology of the Andrews Forest is shaped by volcanism. Areas below 760 m (lower portions of WS 01 and WS 02) are underlain by hydrothermally altered volcanoclastic rocks consisting of massive, reddish and buff-coloured tuffs and breccias derived from mudflows and pyroclastic flows from the Oligocene to early Miocene epochs (33–20 mya). Areas between 760 and 1200 m (upper elevation of WS 01 and WS 02 and lower elevations of MR) are underlain by two units middle to late Miocene (14–5 mya) in age: a lower unit containing welded and non-welded ash flows and an upper ridge-forming unit containing basalt and andesite lava flows. MACK, WS 07, and WS 08 lack a hard ridge-forming unit being predominantly underlain by lava flows

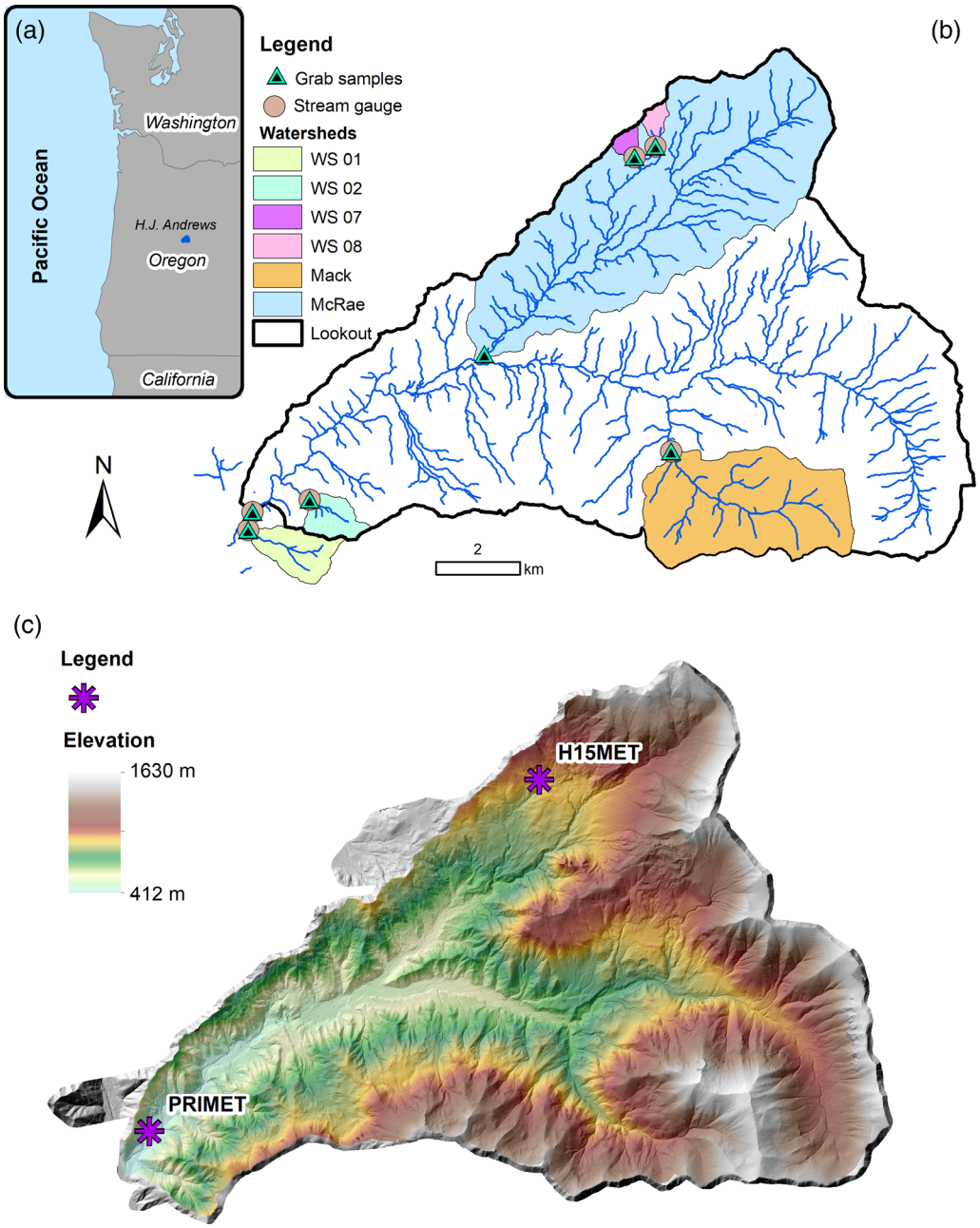

FIGURE 1 (a) Location of the Andrews Experimental Forest, (b) Investigated watersheds and sampling locations for stream grab samples, (c) Elevation from LiDAR and location of precipitation composite samplers

(Swanson & James, 1975). Mean slope gradients exceed 30 deg in WS 01 and WS 02, but slope gradients are ~18 deg in WS 07 and WS 08 (Table 1). Mean slope in MACK is 27 deg while in MR it is 22 deg. More than 80% of precipitation in the Andrews Forest occurs between October and April during long-duration, low-intensity frontal storms (Swanson & Jones, 2002). Mean annual precipitation between 1980 and 2018 was 2193 mm at 436 m.a.s.l (PRIMET station, Figure 1) and 2154 mm at 909 m.a.s.l (H15MET station, Figure 1). WS 01 and WS 02 span the rain to transient snow to seasonal snow zones; WS 07, WS 08, MACK, and MR are in the seasonal snow zone, with a snowpack that can persist from November to late April or June (Harr & McCorison, 1979; Perkins & Jones, 2008; Swanson & Jones, 2002). The physiography of the watersheds was characterized based on the analysis of LiDAR (Spies, 2016) under SAGA-GIS (Conrad et al., 2015) in terms of drainage area, watershed elevation, watershed slope, drainage density, and the index median flow path length over median flow path gradient (L/G) (Table 1).

2.2 | Water stable isotope data collection and analysis

Grab and precipitation water samples were collected between November 2014 and November 2018, over different hydrologic

TABLE 1 Description of physical attributes of study watersheds (WS) and number of water samples collected during the study period 2014–2018. Values in parenthesis represent the mean for elevation and the standatd deviation for slope

WS	Area (ha)	Elevation range (m)	Slope (degrees)	Drainage density (km/km^2)	L/G	Date range	Water samples collected	Water samples used[a]
WS 01	95.9	439–1027 (707)	33.2 (9.5)	2.6	279.8	4 November 2014–13 November 2018	95	77
WS 02	60.7	545–1079 (792)	31.9 (9.5)	2.5	361.6	4 November 2014–13 November 2018	69	56
WS 07	15.4	918–1102 (1011)	19.3 (6.5)	1.0	714.0	4 November 2014–14 November 2018	67	52
WS 08	21.4	962–1182 (1061)	18.2 (7.1)	2.8	640.2	4 November 2014–14 November 2018	70	56
MACK	580	758–1610 (1195)	27.39 (9.2)	2.2	495.6	5 November 2014–14 November 2018	93	77
MR	1500	547–1631 (982)	21.86 (11.0)	3.6	581.0	5 November 2014–14 November 2018	97	81
LOOK	6242	421–1627 (977)	24.4 (11.2)	5.6	515.6	5 November 2014–13 November 2018	92	80

[a]Samples used in the analysis of mean transit time and young water fractions excluded those collected during storm events.

conditions, based on meteorological records at PRIMET and H15MET (Daly & McKee, 2016) and long-term flow records at the investigated watersheds (Johnson et al., 2019). Samples collected in 2015 represented warm conditions with mean winter air temperature 2.5–2.9°C above the average, moderate annual precipitation (357–410 mm below the average), very low snow water equivalent (SWE), which was 87% below the normal value (Figure 2), and mean annual streamflow between the 7th and 12th percentiles. In contrast 2017 was a high-water year with low winter air temperatures (1.6–2.4°C lower than the average), high precipitation (405–581 mm above the average), snow water equivalent 19% above the normal, and mean annual streamflow between the 60th and 81st percentiles (Figure 2). The years 2016 and 2018 fall somewhere in the middle between 2015 and 2017, with air temperatures 0.28–1.1°C above the average in 2016 and 0.4–0.7°C above the average in 2018, precipitation within 100 mm of the means in 2016 and 365–470 mm below the average in 2018; snow water equivalent was 28% lower than the normal in 2016 and it was 50% lower than the normal in 2018. Mean annual streamflow in 2016 was between the 16th and 44th percentile and in 2018, it was between the 14th and 29th percentile.

Grab water samples were collected at the seven watershed outlets on a 3-week basis for a total of 67–97 samples per site (583 samples total) (Segura, 2019). Bulk precipitation samples were collected near two meteorological stations: PRIMET (∼weekly samples) and H15MET

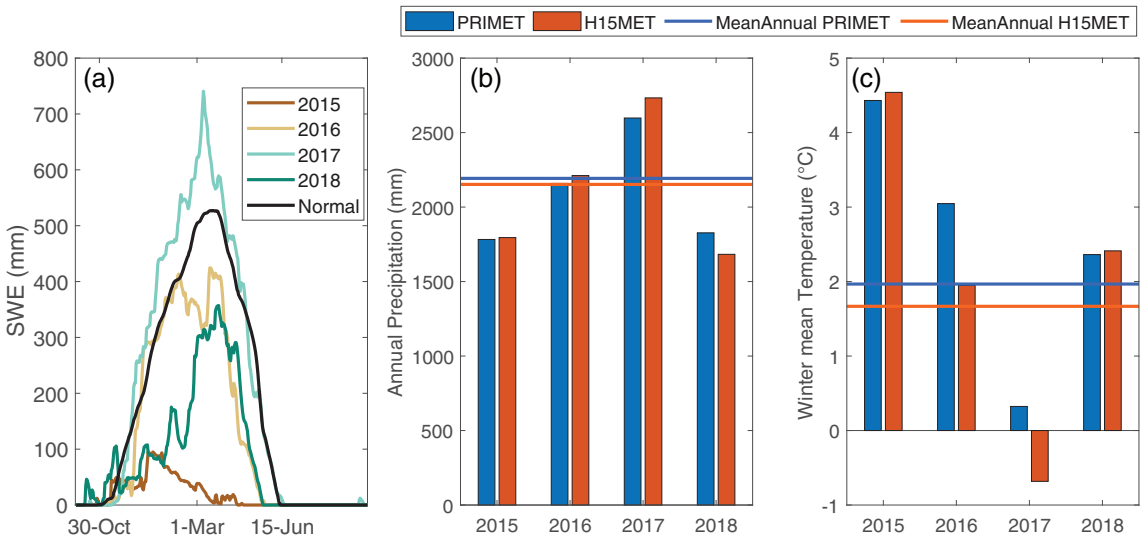

FIGURE 2 Climatic context: (a) Mean daily snow water equivalent (SWE) and 1981–2010 normal across four Snow Telemetry (SNOTEL) Network sites located near the Andrews Forest (Hogg Pass, Jump Off Joe, Mckenzie, Santiam Jct), (b) Annual precipitation at two meteorological stations (Figure 1) (c) Winter (December–February) mean air temperature at two weather stations in the Andrews Forest

(∼samples every 3 weeks) for a total of 153 samples at PRIMET and 60 samples at H15MET (Figure 1) (Segura, 2019). Samples that fell 5‰ or more below the GMWL (32 samples at PRIMET and 7 samples at H15MET) were eliminated as evaporation was likely (Brooks et al., 2012). These 32 samples represented less than 5% of the total precipitation volume in PRIMET and less than 1% of the total precipitation volume in H15MET. Of these 39 samples, 28 were collected during the spring and summer months when storm magnitude is at a minimum and evaporative influences are likely to be strongest.

Precipitation collectors were constructed following IAEA protocols (Groning et al., 2012) to prevent evaporation. Surface water and precipitation samples were sealed in 20 ml screw top glass vials with conical inserts and capped without headspace to prevent isotopic fractionation. Duplicates were collected every 10 samples for quality assurance and control. Samples were stored in dark and cool (<15°C) conditions and analysed at the Watershed Processes Laboratory of Oregon State University.

Water-stable isotopes ratios ($\delta^{18}O$ and $\delta^{2}H$) were measured in all samples using a cavity ring down spectroscopy liquid and vapour isotopic analyser (Picarro L2130–i, Picarro Inc., CA). The samples were ran under the high precision mode, including six injections per sample. The first three injections were discarded to account for memory effects. Two internal (secondary) standards were used to develop calibration curves, while a third internal standard was used to estimate external accuracy. All internal standards were calibrated against the IAEA primary standards for the Vienna Standard Mean Ocean Water (VSMOW2, $\delta^{18}O = 0.0‰$ and $\delta^{2}H = 0.0‰$), Greenland Ice Sheet Precipitation (GISP, $\delta^{18}O = -24.76‰$ and $\delta^{2}H = -189.5‰$), and Standard Light Antarctic Precipitation (SLAP2, $\delta^{18}O = -55.5‰$ and $\delta^{2}H = -427.5‰$). Precision was 0.25‰ and 0.07‰ for $\delta^{2}H$ and $\delta^{18}O$ based on the comparison of 148 duplicated samples. The accuracy of our analyses was 0.26 ± 0.0019‰ and 0.05 ± 0.00029‰ for $\delta^{2}H$ and $\delta^{18}O$ based on the comparison of 104 estimated values to a known internal standard. For the analyses of mean transit time and young water fractions, samples collected during storm events were omitted (Table 1). Eliminating storm samples reduces the weight of measurements during high flow allowing the detection of seasonal fluctuations during baseflow conditions (Lutz et al., 2018; McGuire & McDonnell, 2006; Muñoz-Villers et al., 2016).

2.3 | Data analysis

2.3.1 | Mean transit time

Time invariant mean transit times (MTTs) were estimated using an inverse solution of the lumped convolution approach (Amin & Campana, 1996; Małoszewski & Zuber, 1982) which assumes steady-state conditions (i.e., baseflow MTTs). The convolution approach describes the transit of the input precipitation signal (δ_{in}) to the outlet streamflow signal (δ_{out}) considering a time lag between them $(t-\tau)$. The input precipitation signal was volume weighted so that the outflow composition reflects the mass flux leaving the watershed:

$$\delta_{out}(t) = \frac{\int_0^\infty g(\tau)\, w(t-\tau)\, \delta_{in}(t-\tau)\, d\tau}{\int_0^\infty g(\tau)\, w(t-\tau) d\tau} \quad (1)$$

where τ is the transit time, t is the time of exit from the system, $g(\tau)$ is a transfer function, and $w(t-\tau)$ is the mass weighting factor (McGuire & McDonnell, 2006). The $g(\tau)$ was represented with a gamma distribution with two parameters: α, the shape parameter and β, the scale parameter, and $TT = \alpha \times \beta$. A gamma function has proven effective in a variety of environments to model MTT (Godsey et al., 2010; Hrachowitz et al., 2010; Lutz et al., 2018).

$$g(\tau) = \frac{\tau^{\alpha-1}}{\beta^{\alpha}\Gamma(\alpha)} e^{\left(-\frac{\alpha}{\beta}\right)} \quad (2)$$

The precipitation input was adjusted for elevation effects following the method used by McGuire et al. (2005) considering the two sampling locations (Figure 1). For modelling purposes, the time series of precipitation isotope values in H15MET was filled to match the resolution of samples collected in PRIMET based on the relationship between the two locations (Figure S1). For watersheds influenced by snow (WS 07, WS 08, and MACK) the higher elevation sampling location (H15MET) was used as the reference input signal. For the lower elevation watersheds (WS 01, WS 02, MR, and LOOK) the samples collected at PRIMET were used as the reference input. The input for each modelled period was estimated using linear interpolation based on the difference between the two precipitation stations (see details in McGuire et al. (2005)). Although H15MET is 7 km away from MACK ∼30 composite precipitation water samples collected at MACK between 2015 and 2018 indicated strong relationships between the isotope ratios in samples collected in these two locations (Segura, 2019) (Figure S2).

To evaluate temporal changes in flow routing, MTT was estimated over 53 2-year moving windows spaced every 14 days. The first window started in November 2014 and the last window started in November 2016. In all cases the available isotopic input data was looped 10 times during calibration, similar to previous studies (Capell et al., 2012; Hrachowitz et al., 2010; Hrachowitz et al., 2011; Timbe et al., 2014). Model performance was evaluated using the Nash-Sutcliffe efficiency (NS). Models were built using parameter sets generated through a uniform Monte Carlo sampling procedure (Beven and Freer, 2001). Each model was run >30 000 times over the same parameters ranges for α (0–4) and for β (0–2000) to obtain >100 parameter sets with a NS > 0.2. It was found that 13–51 out of the 53 windows produced solutions with NS > 0.2 across the 7 watersheds for a total of 224 models (Table S1). Across these cases >100 behavioural solutions (i.e., solutions corresponding to at least 95% of the highest NS) (Timbe et al., 2014) were found. The mean and *SD*s of the best parameters α and β and for the MTT were estimated across behavioural model runs.

2.3.2 | Young water fraction

Annual young water fractions were estimated for each watershed following the approximation proposed by Kirchner (2016a) as the amplitude ratio of seasonal sinusoidal models of isotope ratios in precipitation (A_P) and streamflow (A_Q):

$$F_{yw} = \frac{A_Q}{A_P} = \frac{\sqrt{a_Q^2 + b_Q^2}}{\sqrt{a_P^2 + b_P^2}} \quad (3)$$

where the a and b coefficients are obtained by fitting the precipitation and streamflow isotope ratios as:

$$\delta^{18}O_P(t) = \overline{\delta^{18}O_P} + a_P\cos(ct) + b_P\sin(ct) \quad (4a)$$

$$\delta^{18}O_Q(t) = \overline{\delta^{18}O_Q} + a_Q\cos(ct) + b_Q\sin(ct) \quad (4b)$$

where $\delta^{18}O_P(t)$ and $\delta^{18}O_Q(t)$ is the isotopic time value at time t (for P and Q), $\overline{\delta^{18}O_P}$ and $\overline{\delta^{18}O_Q}$ are the mean $\delta^{18}O$ in P and Q, and c is $2\pi/365$ rad/day (Lutz et al., 2018). The values a and b for Q and P were estimated using robust fitting (R statistical software method rml) (Lutz et al., 2018). In order to assess the uncertainty regarding the assumed input signal, two sets of calculations were performed considering volume weighed precipitation input from PRIMET and H15MET. Similarly to von Freyberg et al. (2018), both discharge weighted (F^*_{yw}) and unweighted (F_{yw}) young water fractions were estimated. Uncertainties in the calculated F^*_{yw} and F_{yw} were expressed as *SE* assuming Gaussian error propagation (von Freyberg et al., 2018). To this end 10 000 random samples of the a_P, b_P, a_Q, and b_Q parameters were generated assuming that they follow a normal distribution and estimated the corresponding amplitude ratios.

3 | RESULTS

3.1 | Isotopic composition of precipitation and streamflow

Annual precipitation-weighted isotope ratios between 2014 and 2018 at PRIMET were isotopically heavier than annual precipitation-weighted isotope ratios collected at higher elevation at H15MET (Table 2). However, the differences in isotope ratios were stronger over time. The isotopic ratios in precipitation were heavier in 2015 and lightest in 2017 at both locations (Figure 3a) reflecting difference in snow inputs (Figure 2a) and differences in fractionation rates (Liu et al., 2014; Nusbaumer et al., 2017; Nusbaumer & Noone, 2018; Segura et al., 2019). The local meteorologic water lines (LMWLs) for these two locations are not statistically different with slopes of 8.23 for PRIMET and 8.21 for H15MET and neither of these LMWL are statistically different from the global meteoric water line (GMWL).

Isotope ratios in stream grab samples had a lower variability than precipitation samples and fell around the LMWLs for PRIMET and H15MET (Figure 3b). Overall, there is a decreasing trend in mean annual isotope ratios between 2015 and 2018 for $\delta^{18}O$ (0.04–0.13‰ per year) and for δ^2H (0.1–0.65‰ per year) across all streams (Figure 4). Given the strong correlation between $\delta^{18}O$ and δ^2H (Figure 3b), only $\delta^{18}O$ was used in the modelling of mean transit time and young water fractions.

3.2 | Mean transit time

Modelling provided mean transit time (MTT) results in 224 out of the 371 2-year windows across seven watersheds (Figure S2). Model fits yield mean NS between 0.20 and 0.73 across behavioural solutions with 94 windows having NS above 0.4 (Figure S3). Among all watersheds, the estimated MTT increased between 2015 and 2018 (Figure 5). Mean 2015 MTT varied between 0.9 and 2.0 years while in 2018 MTT varied between 5.0 and 6.0 years (Table 3). The shapes of the MTT distributions were narrow in 2015 while they were wide for all other years (Figure S4). The gamma cumulative probability density functions showed that for 2015 over 60% of the precipitation input travelled to all outlets in less than 555 days (Figure S5). In contrast, for 2018 less than 40% of the precipitation input travelled to the outlet of all watersheds in 462 days (Figure S5).

Overall, the range of estimated MTT (i.e., difference between maximum and minimum MTT across the 4 years) was higher (4.2–4.9 years) for high elevation watersheds (WS 07, WS 08, and MACK) than for the rest of the watersheds (2.1–3.8 years) (Table 3). The MTT in 2016 were longer than the MTT in 2015 across all watersheds, but the differences between these 2 years were larger for the small watersheds (WS 01–WS 08) with 2.1–5.4 times larger MTT in 2016 compared to the MTT in 2015, while in the larger watersheds (MACK, MR, and LOOK) the MTT in 2016 was <3 times larger than the MTT in 2015. In 2016, the MTT in the smaller watersheds (WS 01–WS 08), was significantly longer than the MTT in the larger watersheds (Table S2). In 2017 the MTT estimation was only possible in 4 watersheds with one of the larger watersheds (MR) having significantly shorter MTT than the MTT in smaller watersheds (WS 08 and MACK) (Table S2). In 2018 MTT was not significantly different between watersheds (Table S2), however like in 2017 results were only possible in four watersheds. The MTT calculated considering the available 4-years record varied between 2.4 and 5.8 years (Table 3) but in WS 02 no runs yield NS > 0.2.

The parameters of the gamma function (α and β) change consistently with time. The mean α across watersheds decrease from 2.3 to 1.1 between 2015 and 2018 while on average β increase from 276 in 2015 to 1797 in 2018 (Table S3). High α values were associated to short MTT while low α values were frequent for longer MTT (Table S3). The parameter α was negatively related to snow water equivalent (SWE) ($r = -0.55$, p-value $= 0.0075$), while β was positively related to both annual precipitation ($r = 0.43$, p-value $= 0.04$) and SWE ($r = 0.75$, p-value $= 6.52 \times 10^{-5}$).

TABLE 2 Mean annual magnitude weighted isotope ratios in precipitation bulk samples collected at PRIMET and H15MET and in mean annual isotope ratios in grab samples collected at seven watersheds between 2015 and 2018 (*SD* in parenthesis)

	$\delta^{18}O$ (‰)				$\delta^{2}H$ (‰)			
Watershed/met station	**2015**	**2016**	**2017**	**2018**	**2015**	**2016**	**2017**	**2018**
PRIMET	−9.1 (0.29)	−10.69 (0.45)	−11.22 (0.47)	−10.36 (0.51)	−63.18 (2.37)	−73.97 (3.75)	−77.73 (4.19)	−71.09 (4.40)
H15MET	−9.69 (0.43)	−11.02 (0.28)	−12.6 (0.80)	−11.82 (0.82)	−66.44 (3.62)	−76.55 (2.44)	−89.69 (6.82)	−81.49 (7.09)
WS 01	−10.19 (0.16)	−10.29 (0.2)	−10.64 (0.3)	−10.47 (0.24)	−70.66 (0.16)	−71.45 (0.2)	−73.75 (0.3)	−71.83 (0.24)
WS 02	−10.49 (0.16)	−10.37 (0.15)	−10.64 (0.31)	−10.61 (0.12)	−72.4 (0.16)	−72.1 (0.15)	−73.49 (0.31)	−72.61 (0.12)
WS 07	−11 (0.15)	−10.72 (0.26)	−10.99 (0.14)	−11.06 (0.11)	−75.9 (0.15)	−74.92 (0.26)	−75.8 (0.14)	−75.95 (0.11)
WS 08	−10.65 (0.14)	−10.5 (0.2)	−10.93 (0.18)	−10.88 (0.15)	−73.33 (0.14)	−72.91 (0.2)	−75.07 (0.18)	−74.29 (0.15)
MACK	−10.71 (0.22)	−10.55 (0.29)	−10.99 (0.23)	−11.0 (0.11)	−73.54 (0.22)	−72.76 (0.29)	−75.4 (0.23)	−74.82 (0.11)
MR	−10.59 (0.15)	−10.54 (0.17)	−11 (0.25)	−10.88 (0.15)	−73.15 (0.15)	−72.79 (0.17)	−75.63 (0.25)	−74.27 (0.15)
LOOK	−10.69 (0.24)	−10.57 (0.24)	−11.07 (0.3)	−10.92 (0.24)	−73.95 (0.24)	−73.52 (0.24)	−76.58 (0.3)	−74.7 (0.24)

3.3 | Climatic and physiographic controls of MTT

MTT values were positively correlated to both annual precipitation ($r = 0.44$, p-value $= 0.04$, Figure 6a) and SWE ($r = 0.74$, p-value $= 7.84 \times 10^{-5}$, Figure 6b) indicating shorter transit time during the snow drought in 2015. During 2015 the absolute and relative variability in MTT across watersheds was smaller (SD = 0.39 years, coefficient of variation = 0.32) compared to the variability in MTT during the wetter years of 2016 (SD =1.34 years, coefficient of variation = 0.41) and 2017 (SD = 0.87 years, coefficient of variation = 0.18). Mean annual daily discharge as well as mean daily discharge in the winter and spring explained some of the MTT variability in 2016 ($r = -0.84$ to -0.790, p-value = 0.039–0.06) (Table 4). In addition, there were strong relations between MTT in all years and mean daily discharge in winter ($r = 0.57$ p-value $= 0.01$, Figure 6c) and spring ($r = 0.58$, p-value $= 0.01$, Figure 6d).

The range in MTT in each watershed across the 4 years was positively related to watershed mean elevation ($r = 0.93$, p-value $= 0.0028$), meaning that high elevation watersheds had a wider range in MTT than watersheds located at low elevation. The MTT range was highest in WS 08 (4.9 years) located at 1061 m while the lowest MTT range was calculated for WS 01 (2.1 years), located at 716 m (Table 3). The MTT was negatively correlated to drainage area in 2016 ($r = -0.86$, p-value =0.012, Figure 6e) and 2018 ($r = -0.94$, p-value $= 0.05$, Figure 6e) (Table 4). In contrast MTT during the 2015 drought was unrelated to drainage area ($r = 0.07$, p-value $= 0.88$). This was also the case for the MTT values previously estimated by McGuire et al. (2005) for some of the same watersheds investigated here based on 2001–2002 data (Figure 6e). This is not surprising, considering that 2001 was a dry year with annual precipitation values below 850 mm for the mean annual value at PRIMET and H15MET (Daly & McKee, 2016) (Figure 1).

Analysis of topographic controls on MTT revealed poor correlations between MTT and watershed slope (Table 4). Mean watershed elevation and the index L/G were not correlated to MTT in all years except in 2015 when MTT was inversely related to elevation ($r = -0.83$, p-value $= 0.019$) and L/G was weakly related to MTT ($r = -0.72$, p-value $= 0.066$). Drainage density was inversely related to MTT in 2016 ($r = -0.77$, p-value $= 0.04$). Metrics of terrain roughness (Frankel & Dolan, 2007; Smith, 2014; Wu et al., 2018) explain some of the variability in MTT. The *SD* of elevation was inversely related to MTT in 2016 ($r = -0.83$, p-value =0.018) and 2018 ($r = -0.96$, p-value $= 0.037$) while the *SD* of the slope was weakly related to MTT in 2016 ($r = -0.72$, p-value $= 0.064$, Figure 6f) and strongly related to MTT in 2018 ($r = -0.99$, p-value $= 0.012$, Figure 6f).

3.4 | Fraction of young water

Annual unweighted (F_{yw}) and weighted (F^{*}_{yw}) young water fractions at seven watersheds in the Andrews Forest were similar and varied between 0.04 ± 0.001 and 0.91 ± 0.20 for F^{*}_{yw} and between 0.02

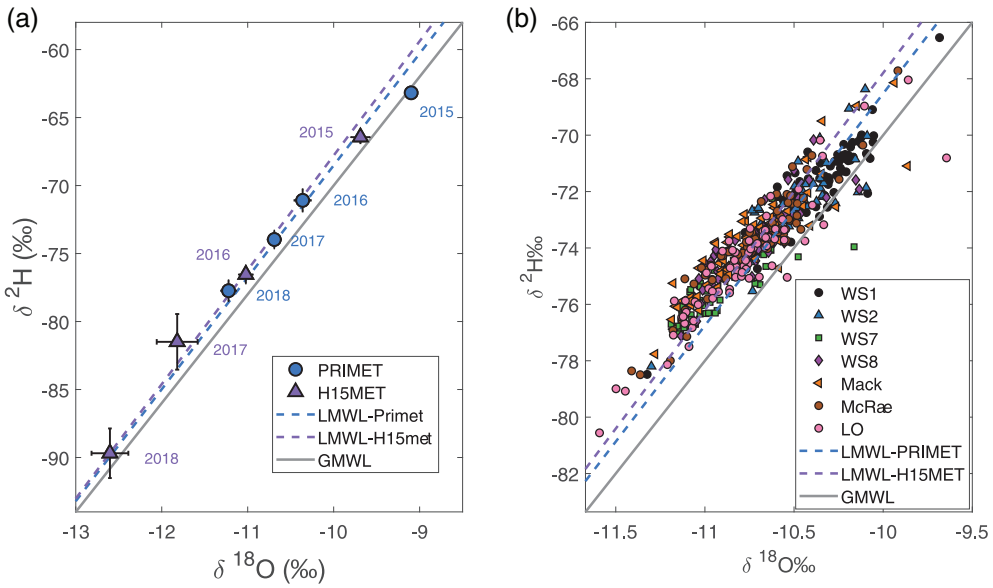

FIGURE 3 (a) Mean annual magnitude weighted isotopic precipitation values in the Andrews Forest at two different elevations (Figure 1) between 2014 and 2018; the local meteoric water lines (LMWLs) were derived based on 121 samples in PRIMET and 53 samples in H15MET. (b) Grab water samples collected at seven locations between 2014 and 2018. The LMWLs and the global meteoric water line (GMWL) are shown for reference

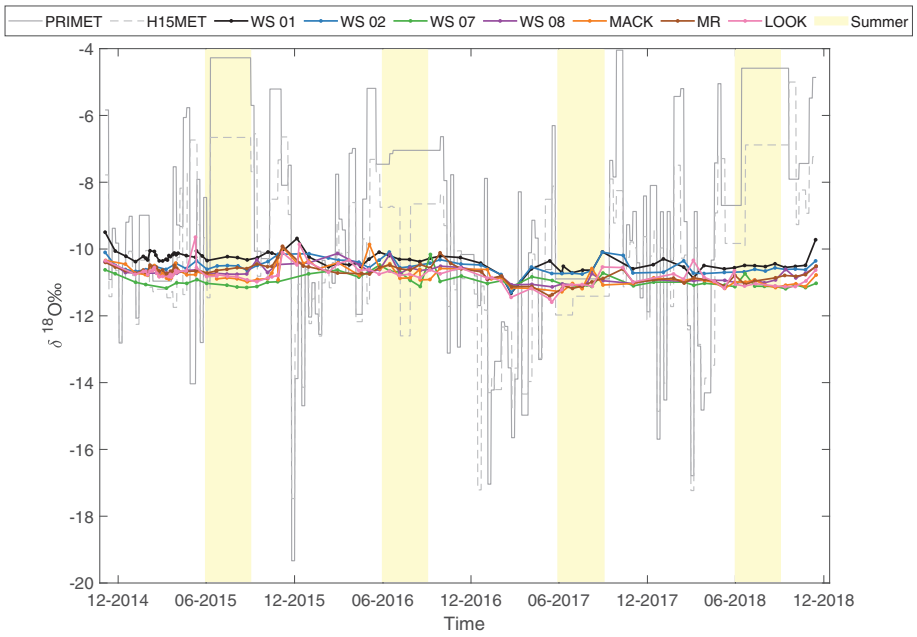

FIGURE 4 $\delta^{18}O$ time series for seven watersheds in the Andrews Forest (Figure 1) during 2014–2018. The grey lines represent $\delta^{18}O$ in precipitation samples at PRIMET and H15MET (Figure 1). The summer/dry period between June and august is highlighted in yellow

± 0.02 and 0.88 ± 0.21 for F_{yw} (Tables 5 and S4). As previous studies have reported, F_{yw} and F^*_{yw} were correlated ($r = 0.77$, p-value $= 9.63 \times 10^{-6}$) resulting generally in higher F^*_{yw} than F_{yw} (von Freyberg et al., 2018). Weighted young water fractions estimated based on data collected at the higher elevation meteorological station, H15MET yield similar results to those estimated based on precipitation data from PRIMET indicating higher F^*_{yw} for 2015 compared to any other year (Figure S6) indeed the two estimates of F^*_{yw} are correlated ($r = 0.99$, p-value $= 4.4 \times 10^{-25}$). Given these results (i.e., strong relations between F_{yw} and F^*_{yw} and between F^*_{yw} estimated using data from the two meteorological stations) the analysis of controlling factors of young water fractions using any of these estimates would be very similar. The analysis below is based on weighted young water fractions (F^*_{yw}) estimated based on PRIMET data.

The variability in F^*_{yw} was larger over time —year to year— than over space —across watersheds. On average across watersheds F^*_{yw} was the largest in 2015 (mean = 0.49, SD = 0.24) and smallest in 2016 (mean = 0.08, SD = 0.04) (Table 5). The mean 2015 F^*_{yw} was significantly higher than the mean F^*_{yw} in 2016, 2017 and 2018 (Table S5). The mean F^*_{yw} values in 2016, 2017 and 2018 were not statistically different (Table S5).

3.5 | Climatic and physiographic controls in young water fraction

Considering all the data, the F^*_{yw} was negatively correlated to April 1st snow water equivalent ($r = -0.63$, p-value $= 3.23 \times 10^{-4}$,

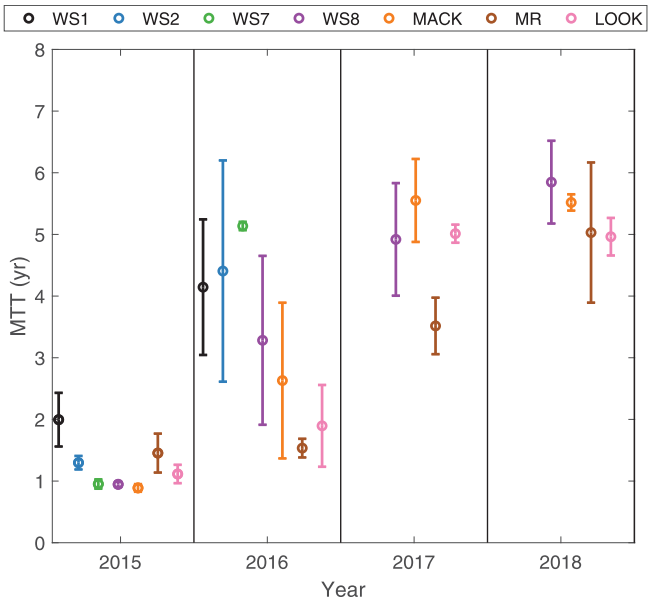

FIGURE 5 Mean annual MTT for seven watersheds in the Andrews Forest (Figure 1). Each point and bar represent the mean and *SD* of the MTT estimated across 13–14 2-year windows spaced every 2 weeks around the year of interest (Table 3)

Figure 7a). However, excluding the 2015 data the relationship between F^*_{yw} and SWE was positive ($r = 0.51$, p-value $= 0.018$). The F^*_{yw} was also positively correlated to total precipitation if the data from 2015 is excluded ($r = 0.49$, p-value $= 0.025$) (Figure 7b). The F^*_{yw} varied greatly in 2015 between 0.17 and 0.91 with the largest F^*_{yw} values (0.61–0.91) calculated for small watersheds located at high elevation (WS 07 and WS 08, Table 5). These watersheds received much lower snow amounts in 2015 than normal (Figure 2). In 2018 the variability in F^*_{yw} was smaller between 0.05 and 0.2 (Table 5). While mean annual daily streamflow was not correlated to F^*_{yw}variability (Table 4). There were strong inverse relations between F^*_{yw} in all years and mean daily discharge in the winter ($r = -0.52$, p-value $= 0.009$) (Figure 7c).

Drainage area was positively correlated to F^*_{yw} in 2018 ($r = 0.84$, p-value $= 0.017$, Table 4, Figure 7e) but unrelated to F^*_{yw} in all other years. Mean watershed slope and elevation were uncorrelated to F^*_{yw} (Table 4). However, the *SD* of elevation was positively related to F^*_{yw} in 2018 ($r = 0.8$, p-value $= 0.025$, Table 4). The index L/G was weakly correlated to F^*_{yw} in 2017 ($r = -0.70$, p-value $= 0.077$ Table 4) and drainage density was weekly related to F^*_{yw} in 2018 ($r = 0.72$, p-value $= 0.066$, Table 4). Metrics of terrain roughness explain some of the variability in F^*_{yw}. The *SD* of elevation was positively related to F^*_{yw} in 2018 ($r = 0.82$, p-value $=0.025$, Table 4) while the *SD* of the slope was negatively related to F^*_{yw} in 2015 ($r = -0.77$, p-value $= 0.042$, Figure 7f) and positively related to F^*_{yw} in 2018 ($r = -0.75$, p-value $= 0.047$, Figure 7f). In 2017 the *SD* of the slope was weakly related to F^*_{yw} ($r = 0.69$, p-value $= 0.085$, Figure 7f).

4 | DISCUSSION

4.1 | Spatial and temporal variability of mean transit time

The results demonstrate that both extrinsic controls and intrinsic watershed characteristics influence mean transit time (MTT) variability in the Andrews Forest. The wide range on climatic conditions analysed here, including the 2015 snow drought, resulted in MTT values that varied over time with snow input and across space with physiography apparently mediated by moisture level. During the snow drought in 2015, MTT was significantly shorter compared to the MTT in any other subsequent year. The differences in MTT across moisture levels were also reflected in the variability of the alpha parameter of the gamma function which was inversely related to snow water equivalent. The shorter MTT during the drought contrast previous analysis for mountainous watersheds in Pennsylvania (McGuire et al., 2002), humid systems in Scotland (Birkel et al., 2012; Hrachowitz et al., 2009), boreal systems in Europe (Peralta-Tapia et al., 2016), and cold prairie watersheds in North America (Bansah & Ali, 2019) in all of which longer MTT were associated to dry conditions and shorter MTT were related to wet conditions. The shorter MTT during 2015 indicate that during this unprecedent snow drought (Mote et al., 2018; Segura et al., 2019) the active flow paths were short and unconnected to older stored water. One could envision that in 2015 most of the water that contribute to baseflow moved primarily horizontally with limited vertical mixing between surface water and older ground water sources (Kleine et al., 2020). The climatic conditions in 2015 were dramatic in terms of snowpack inputs which were practically absent in the region (Mote et al., 2018). In the absence of the snow, soil moisture likely declined dramatically which could have limited ground water recharge. I pose that the short transit times observed in 2015 resulted from the low connectivity between surface water in the streams and older subsurface water. Thus, the absence of a snowpack appears to have led to short transit times. Furthermore, the prolonged summer in this region, with negligible water inputs, during more than 3 months exacerbated the hydrologic disconnection resulting in a relatively homogenous hydrologic response across all the investigated watersheds with MTT shorter than 2 years during 2015.

The low variability in MTT during 2015 also infers that the influence of geology and geomorphology at controlling different residence times was limited during the drought when all streams were fed by relatively young water sources. During the 2015 drought, water isotopes in the streams were lighter (more depleted) than the mean incoming precipitation, indicating that water draining at the outlet of the investigated watersheds was a likely a combination of recent precipitation and water stored in geomorphic features (Segura et al., 2019) that on average was less than 2 years old as all 2015 MTT were shorted than 2 years. Given the more depleted stream isotope ratios in 2015 compared to the precipitation, the water in the streams was likely not only relatively young (1–2 years) but also supported in part by high elevation snowmelt that could have been

TABLE 3 Mean annual mean transit time (MTT) and Nash–Sutcliffe efficiency (NS) calculated in 13–14 2-year windows per year. The *SD* across behavioural runs (with an NS > the 95th percentile of all simulations with NS > 0.2) is in parenthesis

WS	2015		2016		2017		2018		All data (4 years)	
	MTT (years)	NS	MTT (years)	NS	MTT (years)	NS	MTT (years)	NS	MTT (years)	NS
WS 01	1.99 (0.44)	0.55 (0.13)	4.14 (1.1)	0.39 (0.12)					4.29 (0.8)	0.35 (0.005)
WS 02	1.3 (0.11)	0.32 (0.09)	4.41 (1.79)	0.23 (0.01)					5.76 (1.7)	0.09 (0.001)
WS 07	0.95 (0.08)	0.27 (0.02)	5.14 (0.07)	0.23 (0.01)					5.71 (1.04)	0.21 (0.003)
WS 08	0.95 (0.04)	0.33 (0.09)	3.28 (1.37)	0.48 (0.04)	4.92 (0.91)	0.41 (0.13)	5.85 (0.67)	0.36 (0.11)	3.61 (0.89)	0.48 (0.007)
MACK	0.89 (0.06)	0.25 (0.05)	2.63 (1.26)	0.35 (0.03)	5.55 (0.67)	0.24 (0.02)	5.52 (0.13)	0.26 (0.05)	3.49 (0.85)	0.4 (0.005)
MR	1.45 (0.32)	0.45 (0.15)	1.53 (0.15)	0.76 (0.06)	3.52 (0.46)	0.59 (0.17)	5.03 (1.14)	0.35 (0.16)	2.38 (0.56)	0.4 (0.01)
LOOK	1.11 (0.15)	0.29 (0.02)	1.9 (0.66)	0.55 (0.1)	5.01 (0.15)	0.33 (0.04)	4.96 (0.3)	0.28 (0.06)	2.71 (0.92)	0.35 (0.005)

Note: The mean MTT per year included MTT estimated over 13–14 2-year windows: For 2015, the windows varied between November-2014 and May-2017. For 2016, the windows varied between May-2015 and November-2017. For 2017, the windows varied between November-2015 and May-2018. For 2018, the windows varied between May-2016 and November-2018.

received during the previous winter snowpack and travelled through subsurface flow paths in less than 2 years. This was likely a hydrologic mechanism for high elevation watersheds (WS 07, WS 08, and MACK) which normally receive precipitation as snow that can persist in the ground from November to June (Harr & McCorison, 1979; Perkins & Jones, 2008; Swanson & Jones, 2002) and are underlain by porous and permeable young volcanic bedrock (Brooks et al., 2012; McGill et al., 2021; Segura et al., 2019; Tague et al., 2013; Tague & Grant, 2004). In years with a snowpack (2016–2018), the MTT was longer draining flow paths connected to water that had been stored in the systems for 1.5–6 years. That is, longer flow paths appear to be active in years with snow.

Although the temporal variability in MTT was higher than its spatial variability, intrinsic watershed characteristics such as drainage area and terrain roughness influence MTT variability to some extent. Similarly, to other studies, the importance of such physiographic variables is mediated by moisture conditions (Heidbuchel et al., 2013). For example, the control that watershed slope has on subsurface water movement depends on moisture condition and increases with watershed wetness both in snowmelt dominated systems (Leach et al., 2020) and small mountainous watersheds (Woods & Rowe, 1996). For the investigated watersheds, the relation between drainage area and MTT was weaker during dry conditions consistent with previous results in the Andrews Forest (McGuire et al., 2005). However, weak relationships between MTT and drainage area have also been reported with no apparent connection to moisture level (Bansah & Ali, 2019; Lane et al., 2020; McGlynn et al., 2003; Rodgers et al., 2005). Consistent with the idea of moisture mediated controls of physiography on MTT, strong relations were found between terrain roughness (*SD*s of the slope and elevation) and MTT in 2016 and 2018. However, these relations were absent in the wettest year of 2017 for which results were only achieved in 4 of the 7 watersheds. Although topography can affect groundwater flow by driving depth to bedrock and flow gradients (Mueller et al., 2013; Mwakalila et al., 2002; Price, 2011; Segura et al., 2019; Warix et al., 2021) the results represented here showed that when conditions are dry with presumably limited ground water recharge from snowmelt, water systems might become disconnected to the older ground water. This is likely the case because soil water storage plays a major role in controlling hydrologic partitioning by activating and deactivating prevalent flow paths (Heidbuchel et al., 2013).

4.2 | Spatial and temporal variability of young water fractions

Young water fractions varied both in space and time being higher during the 2015 snow drought when on average 49% of the water in the investigated watershed outlets was received 2–3 months prior. The mean young water fractions in 2015 in this study were higher than mean values reported for many small streams in Europe (Ceperley et al., 2020; Dimitrova-Petrova et al., 2020; Lutz et al., 2018; von Freyberg et al., 2018) and similar to young water fractions reported

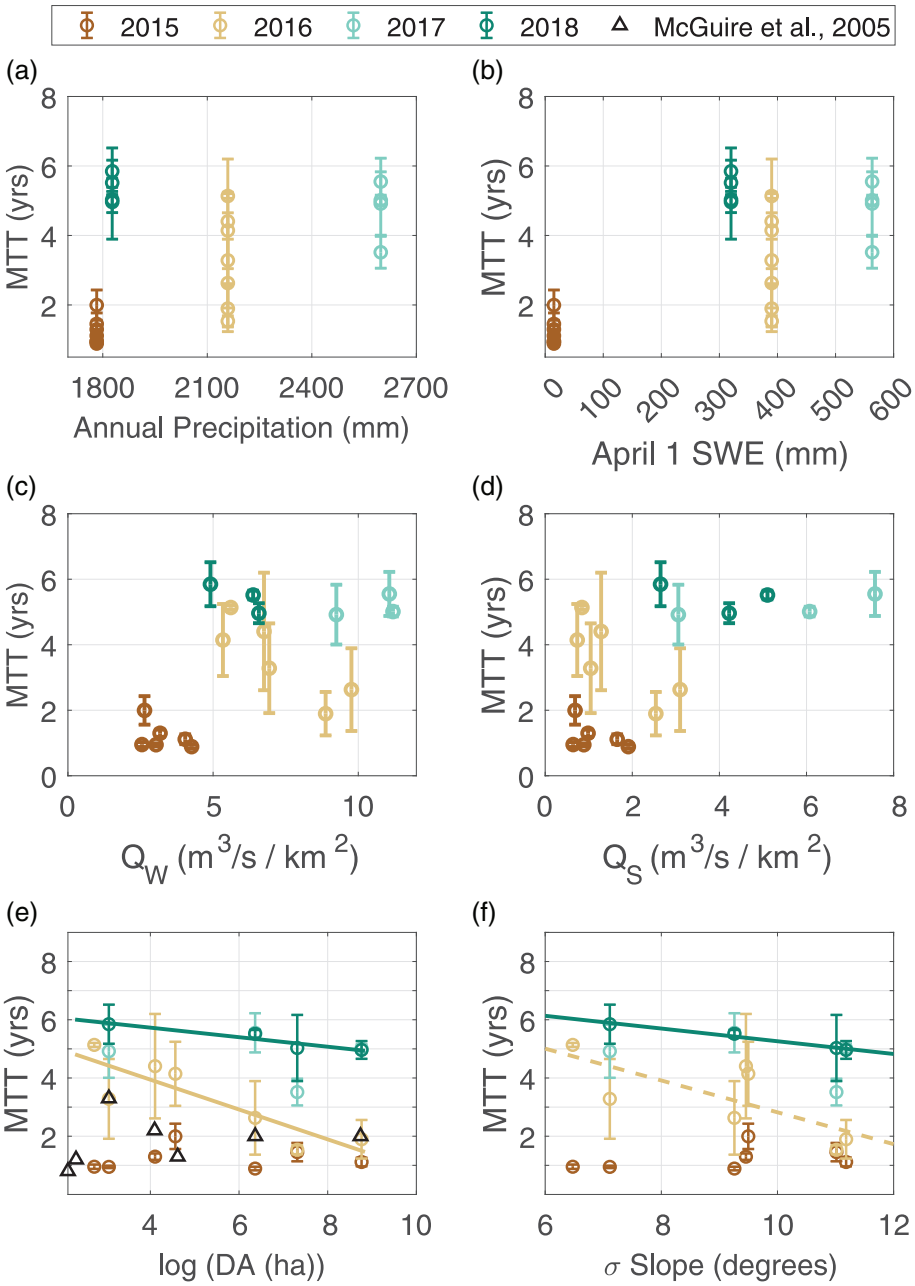

FIGURE 6 Relationship between mean transit time (MTT) and (a) Mean annual precipitation, (b) April 1st snow water equivalent (SWE), (c) Mean daily winter discharge, (d) Mean daily spring discharge, (e) Drainage area (DA), and (f) *SD* of water slope (σ slope). A solid line indicates a relationship with a *p*-value <0.05 and a dash line indicates a relationship with a *p*-values between 0.05 and 0.1

for cold prairie watersheds (Bansah & Ali, 2019) and high elevation watersheds in the Alps (Schmieder et al., 2019). The fractions of young water between 2016 and 2018 were significantly smaller than in 2015 and closer in magnitude to those reported in the mentioned European sites, indicating that 4%–29% of the water in the streams was 2–3 months old. Like in this study, others have reported time variability in young water fractions (Stockinger et al., 2019) with higher uncertainty being associated to warmer/drier conditions. The larger young water fractions found in 2015 compared to the other 3 years is somewhat surprising as many have found lower proportions or young water fractions during dry conditions when presumably older ground water sources feed streams (Bansah & Ali, 2019). However, like in our case, a study including 24 watersheds in Germany reported an inverse relation between precipitation and young water fractions (Lutz et al., 2018). The conditions in 2015 were dramatic in terms of snow inputs with the lowest regional average of April 1st SWE in the available record (1930–2019) (Crampe et al., 2021). The lack of snow in 2015 led to reduce hydrologic connectivity that effectively limited water age at the stream outlets. As mentioned before, in 2015 on average half of the water in the streams was only 2–3 months old and possibly sourced from water stored in geomorphic features (Segura et al., 2019). Part of baseflow in 2015 could have also been sourced from high elevation snowpack received the year before which travel in the subsurface unconnected to older sources as indicated by the short MTT in 2015. In years with a snowpack (2016–2018) longer flow paths are active leading to longer transit times that incorporate water stored in the watersheds for >2 years and that results in higher winter daily flows. Similar to other studies (von Freyberg et al., 2018),

TABLE 4 Pearson correlations (*p*-value in parenthesis) between mean transit time (MTT) and young water fraction (F^*_{yw}) and drainage area (DA), mean watershed slope (S), *SD* of the slope (σS), mean watershed elevation (H), *SD* of the elevation (σH), drainage density (DD), index L/G, mean annual daily discharge (Q_A), mean daily winter discharge (Q_W), and mean daily spring discharge (Q_S)

	Year	DA	S	σ S	H	σ H	DD	L/G	Q_A	Q_W	Q_S
MTT	2015	0.07 (0.876)	0.62 (0.135)	0.41 (0.357)	−0.83 (0.019)[a]	0.16 (0.726)	0.1 (0.825)	−0.72 (0.066)[b]	−0.26 (0.619)	−0.256 (0.624)	−0.26 (0.619)
	2016	−0.86 (0.012)[a]	0.2 (0.661)	−0.73 (0.064)[b]	−0.4 (0.371)	−0.84 (0.018)[a]	−0.77 (0.042)[a]	−0.09 (0.849)	−0.823 (0.044)	−0.835 (0.039)[a]	−0.792 (0.06)[b]
	2017	−0.17 (0.825)	0.46 (0.537)	−0.41 (0.588)	0.69 (0.312)	−0.28 (0.72)	−0.2 (0.797)	−0.44 (0.559)	0.697 (0.509)	−0.27 (0.826)	0.116 (0.926)
	2018	−0.94 (0.05)[a]	−0.35 (0.653)	−0.99 (0.012)[a]	0.62 (0.384)	−0.96 (0.037)[a]	−0.76 (0.244)	0.48 (0.523)	−0.614 (0.579)	−0.865 (0.335)	−0.544 (0.634)
	2015–2018	−0.67 (0.101)	0.36 (0.426)	−0.46 (0.301)	−0.48 (0.273)	−0.63 (0.13)	−0.52 (0.231)	−0.24 (0.597)	NA	NA	NA
F^*_{yw}	2015	−0.5 (0.256)	−0.51 (0.247)	−0.77 (0.042)[a]	0.36 (0.432)	−0.59 (0.167)	−0.4 (0.38)	0.61 (0.142)	−0.428 (0.397)	−0.261 (0.617)	−0.234 (0.655)
	2016	−0.08 (0.857)	0.39 (0.383)	0.05 (0.912)	−0.49 (0.266)	−0.09 (0.851)	0.1 (0.829)	−0.55 (0.203)	−0.277 (0.595)	−0.356 (0.489)	−0.335 (0.516)
	2017	0.54 (0.212)	0.55 (0.203)	0.69 (0.085)[b]	−0.44 (0.328)	0.56 (0.19)	0.57 (0.181)	−0.71 (0.077)[b]	0.294 (0.572)	0.173 (0.743)	0.181 (0.732)
	2018	0.84 (0.017)[a]	0.34 (0.454)	0.76 (0.047)[a]	−0.08 (0.863)	0.82 (0.025)[a]	0.72 (0.066)[b]	−0.39 (0.387)	0.59 (0.218)	0.636 (0.174)	0.506 (0.305)

[a]These values indicates a correlation with a *p*-value <0.05.
[b]These values indicates a correlation with a *p*-value between 0.05 and 0.1.

strong relations were found between young water fractions and winter mean daily discharge. Large mean daily discharge values are associated to low young water fractions and low mean daily winter discharge was associated to high young water fractions.

4.3 | Effects of the 2015 drought in water movement

Evidence from two transit time metrics indicated that during extreme snow drought conditions in mountainous streams flow paths were short resulting in short MTT and large young water fractions. Limited vertical connectivity between surface and ground water could be a mechanism that contribute to the shorter transit times. The results also indicate that during 2015 snowpack contributions from the previous years could have been important particularly in the high elevation watersheds in which subsurface water movement is possible though porous lava deposits (Swanson & James, 1975). The flow paths that were active in 2015 likely connected water stored in geomorphic features such deep-seated earthflows and other Quaternary deposits (Segura et al., 2019) for less than 2 years. The short transit times in 2015 are despite the presence of at least one spring—Cold Creek—in the Andrews Forest that has been shown to contribute a significant proportion of the flow during the summer conditions both during drought and normal conditions (Segura et al., 2019). Although, there is uncertainty associated with the two metrics (see section below), the fact that they independently indicated that during the snow drought transit times were short adds validation of our results. Although dry conditions resulted in short transit times in all watersheds, the impacts were higher for small streams at high elevation that depend on snowmelt inputs. Shorter transit times during the drought have implications for water quality and solute concentrations as biogeochemical processes are controlled in part by the time water resides and interacts within the subsurface (Gómez-Gener et al., 2020; Hrachowitz et al., 2015; Laudon & Sponseller, 2017; Sebestyen et al., 2014; Wymore et al., 2017). Thus, although the impacts of the drought on short MTT appeared to be short lived, further research is needed to understand long-terms effects on water quality. With snowpack continuing to decline as climate warms in the western United States (Mote et al., 2005), our results underscore the importance of long-term observations that include extreme conditions and the need to further investigate the relevance of water storage in varying geology and geomorphology features (Segura et al., 2019) to modulate water sources during different seasons.

4.4 | Limitations in the approach

The MTT estimates calculated with a convolution approach are limited to represent baseflow transit time distributions. These estimates are thus stationary and do not represent rapidly changing water flow paths and velocities in response to hydrologic forcing (Birkel et al., 2012; Heidbuechel et al., 2012; Hrachowitz et al., 2010;

TABLE 5 Values ± *SE* of flow weighted annual amplitude coefficients of stream water isotopes (As) and flow-weighted young water fractions (F^*_{yw}) at seven watersheds (WS)

	As ± SE (‰)				F^*_{yw} ± SE (−)			
WS	2015	2016	2017	2018	2015	2016	2017	2018
WS 01	0.12 ± 0.07	0.62 ± 0.15	0.67 ± 0.19	0.15 ± 0.07	0.32 ± 0.21	0.17 ± 0.04	0.29 ± 0.08	0.14 ± 0.07
WS 02	0.15 ± 0.07	0.16 ± 0.03	0.32 ± 0.13	0.07 ± 0.01	0.39 ± 0.2	0.04 ± 0.01	0.14 ± 0.06	0.07 ± 0.01
WS 07	0.35 ± 0.02	0.16 ± 0	0.13 ± 0.1	0.07 ± 0.002	0.91 ± 0.2	0.04 ± 0	0.05 ± 0.04	0.06 ± 0.01
WS 08	0.23 ± 0.03	0.36 ± 0.16	0.34 ± 0.03	0.05 ± 0.003	0.61 ± 0.16	0.1 ± 0.04	0.15 ± 0.01	0.05 ± 0.01
MACK	0.18 ± 0.03	0.23 ± 0.08	0.39 ± 0.06	0.13 ± 0.07	0.47 ± 0.13	0.06 ± 0.02	0.17 ± 0.03	0.12 ± 0.06
MR	0.06 ± 0.04	0.2 ± 0	0.45 ± 0.04	0.12 ± 0.05	0.17 ± 0.1	0.05 ± 0	0.2 ± 0.02	0.11 ± 0.05
LOOK	0.21 ± 0.04	0.28 ± 0.09	0.52 ± 0.05	0.21 ± 0.05	0.54 ± 0.15	0.08 ± 0.03	0.22 ± 0.02	0.2 ± 0.05

Note: Magnitude-weighted amplitude coefficients of precipitation (AP) for PRIMETE = 0.38 ± 0.08 in 2015; 3.71 ± 0.13 in 2016; 2.31 ± 0.09 in 2017 and 1.09 ± 0.15 in 2018.

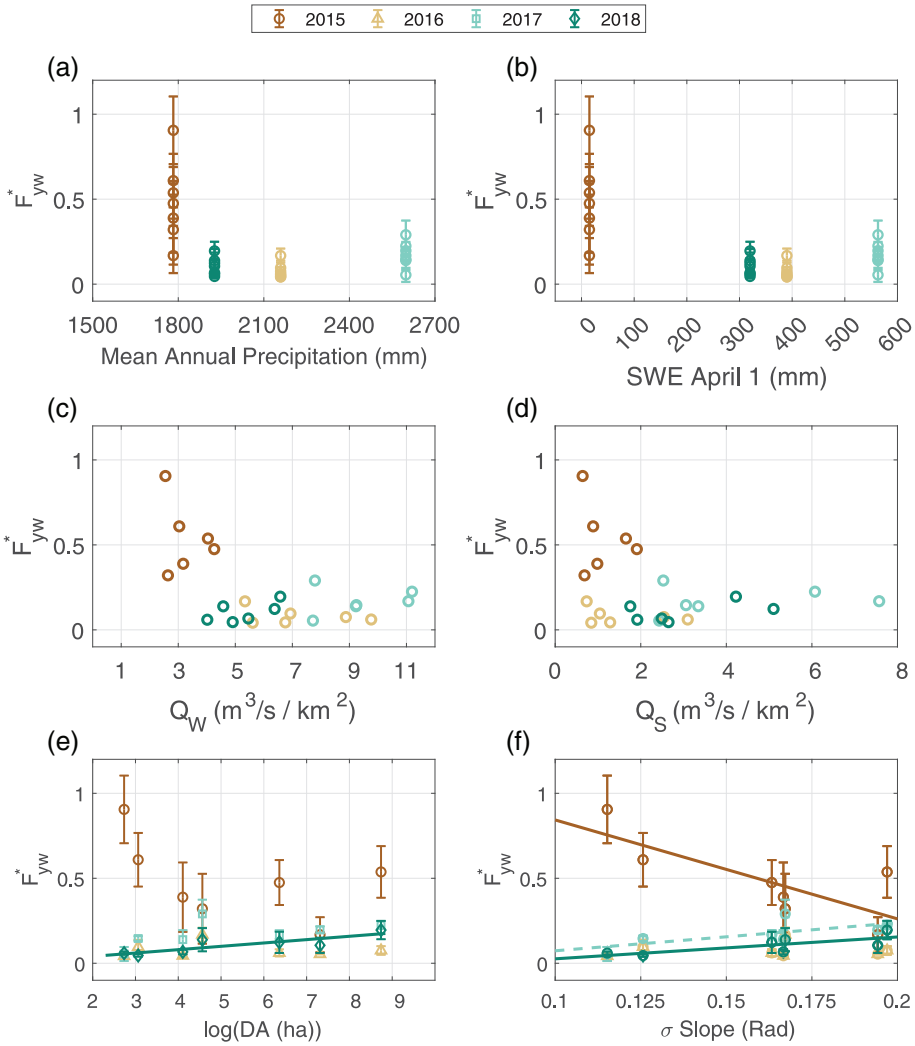

FIGURE 7 Relationship between young water fraction (F^*_{yw}) and (a) Mean annual precipitation, (b) April 1st snow water equivalent (SWE), (c) Mean daily winter discharge, (d) Mean daily spring discharge, (e) Drainage area (DA), and (f) *SD* of water slope (σ slope). A solid line indicates a relationship with a *p*-value <0.05 and a dash line indicates a relationship with a *p*-values between 0.05 and 0.1

Kirchner et al., 2000; Tetzlaff et al., 2007). The failure of the convolution approach to generate estimates of MTT in 2017 and 2018 in three of the investigate watersheds could indicate the dominance of rapidly changing flow paths in these smaller watersheds during wet conditions. Another possible explanation for the lack of model convergence is that the MTT in some of these watersheds is too long to be capture using conservative tracers (Stewart et al., 2010). This could be the case for WS 02 in which the MTT estimation using the 4-year data

record did not yield behavioural solutions. Future work should consider long-term high-resolution data in these systems to explore the importance of rapid changing flow paths.

The uncertainty in young water fractions estimates can be associated the choice of weighting or not weighting the output tracer signal and the choice of input signal (i.e., elevation of the input). Undistinguishable results were found considering weighted or unweighted output signals as well as considering the input signals from two different elevations. Finally, as others have pointed out (Bansah & Ali, 2019) assuming a one-year cycle fit could have underestimated the true amplitudes of both the input precipitation (Ap) and the output streamflow (As). In that sense the results are more robust in terms of the relative comparison between years than in terms of the absolute values found for the fractions of young water. High resolution-long-term data is critical to understand why in some watershed such as WS 01 and MR the young water fractions in 2017 (the highest snow year) were so close to the young water fractions during the 2015 snow drought.

5 | CONCLUSIONS

The analysis of annual variability in transit over 4 years revealed drastic differences between the 2015 snow drought and all other years. During 2015, all the investigated waterheads responded similarly with short transit times. I pose that in the absence of substantial snowpack hydrologic connectivity is impaired. This leads to low flows that are sourced from sources that are not mixed with ground water older than 2 years. The relatively homogenous response in 2015 across the landscape indicated that the importance of intrinsic watershed characteristics such as terrain slope diminishes during dry conditions. Although the impacts of the drought in MTT and young water fractions appeared to be short lived, further research is needed to understand long-terms effects of the reduction of transit times as it relates to flow permanence and stream habitat and to water quality. With snowpack continuing to decline, long term sampling of isotope tracers across experiment watersheds is critical to inform changes in hydrologic behaviour.

ACKNOWLEDGEMENTS

This study was funded by the National Science Foundation Grant No. 1943574 and by the USDA National Institute of Food and Agriculture-McIntire Stennis Project OREZ-FERM-876. Streamflow and temperature data were provided by the HJ Andrews Experimental Forest and Long-Term Ecological Research (LTER) program, administered cooperatively by the USDA Forest Service Pacific Northwest Research Station, Oregon State University, and the Willamette National Forest. This material is based upon work supported by the National Science Foundation under the LTER Grants LTER7 DEB-1440409 (2012–2020) and LTER8 DEB-2025755 (2020–2026). I thank Renee Brooks, Julia Jones, and F.J. Swanson for helpful discussions; Emily Crampe for help in the laboratory; Arianna Goodman for help coding, and Greg Downing and Mark Schulze for assistance collecting samples.

DATA AVAILABILITY STATEMENT

Streamflow and temperature data were provided by the HJ Andrews Experimental Forest and Long-Term Ecological Research (LTER) program, administered cooperatively by the USDA Forest Service Pacific Northwest Research Station, Oregon State University, and the Willamette National Forest. This material is based upon work supported by the National Science Foundation under the LTER Grant LTER7 DEB-1440409 (2012–2020) and LTER8 DEB–2025755 (2020–2026). Isotopic data are available ad the HJ Andrews Experimental Forest database under entry HF028.

ORCID

Catalina Segura https://orcid.org/0000-0002-0924-1172

REFERENCES

Amin, I. E., & Campana, M. E. (1996). A general lumped parameter model for the interpretation of tracer data and transit time calculation in hydrologic systems. *Journal of Hydrology*, *179*(1-4), 1–21. http://doi.org/10.1016/0022-1694(95)02880-3

Bansah, S., & Ali, G. (2019). Streamwater ages in nested, seasonally cold Canadian watersheds. *Hydrological Processes*, *33*, 495–511.

Benettin, P., Rinaldo, A., & Botter, G. (2015). Tracking residence times in hydrological systems: Forward and backward formulations. *Hydrological Processes*, *29*, 5203–5213.

Benettin, P., Soulsby, C., Birkel, C., Tetzlaff, D., Botter, G., & Rinaldo, A. (2017). Using SAS functions and high-resolution isotope data to unravel travel time distributions in headwater catchments. *Water Resources Research*, *53*, 1864–1878.

Birkel, C., Soulsby, C., Tetzlaff, D., Dunn, S., & Spezia, L. (2012). High-frequency storm event isotope sampling reveals time-variant transit time distributions and influence of diurnal cycles. *Hydrological Processes*, *26*, 308–316.

Botter, G., Bertuzzo, E., & Rinaldo, A. (2010). Transport in the hydrologic response: Travel time distributions, soil moisture dynamics, and the old water paradox. *Water Resources Research*, *46*(W03514). https://doi.org/10.1029/2009WR008371

Botter, G., Bertuzzo, E., & Rinaldo, A. (2011). Catchment residence and travel time distributions: The master equation. *Geophysical Research Letters*, *38*, L11403. https://doi.org/10.1029/2011GL047666.

Brooks, J. R., Wigington, P. J., Phillips, D. L., Comeleo, R., & Coulombe, R. (2012). Willamette River Basin surface water isoscape (δ18O and δ2H): temporal changes of source water within the river. *Ecosphere*, *3*(5), art39. http://doi.org/10.1890/es11-00338.1

Campbell, É. M. S., Pavlovskii, I., & Ryan, M. C. (2020). Snowpack disrupts relationship between young water fraction and isotope amplitude ratio; approximately one fifth of mountain streamflow less than one year old. *Hydrological Processes*, *34*, 4762–4775.

Capell, R., Tetzlaff, D., Hartley, A. J., & Soulsby, C. (2012). Linking metrics of hydrological function and transit times to landscape controls in a heterogeneous mesoscale catchment. *Hydrological Processes*, *26*, 405–420.

Ceperley, N., Zuecco, G., Beria, H., Carturan, L., Michelon, A., Penna, D., Larsen, J., & Schaefli, B. (2020). Seasonal snow cover decreases young water fractions in high alpine catchments. *Hydrological Processes*, *34*, 4794–4813.

Conrad, O., Bechtel, B., Bock, M., Dietrich, H., Fischer, E., Gerlitz, L., Wehberg, J., Wichmann, V., & Böhner, J. (2015). System for automated

Geoscientific analyses (SAGA) v. 2.1.4. *Geoscientific Model Development*, *8*, 1991–2007.

Crampe, E. A., Segura, C., & Jones, J. A. (2021). Fifty years of runoff response to conversion of old-growth forest to planted forest in the H. J. Andrews Forest, Oregon, USA. *Hydrological Processes*, *35*(5), e14168. http://doi.org/10.1002/hyp.14168

Daly, C., & McKee, W. A. (2016). Meteorological data from benchmark stations at the Andrews Experimental Forest, 1957 to present. Long-Term Ecological Research. Forest Science Data Bank, Corvallis, OR (4 November 2018) Available: http://andlter.forestry.oregonstate.edu/data/abstract.aspx?dbcode=MS001

Dimitrova-Petrova, K., Geris, J., Wilkinson, M. E., Lilly, A., & Soulsby, C. (2020). Using isotopes to understand the evolution of water ages in disturbed mixed land-use catchments. *Hydrological Processes*, *34*, 972–990.

Frankel, K. L., & Dolan, J. F. (2007). Characterizing arid region alluvial fan surface roughness with airborne laser swath mapping digital topographic data. *Journal of Geophysical Research*, *112*(F2), http://doi.org/10.1029/2006jf000644

Gabrielli, C. P., & McDonnell, J. J. (2020). Modifying the Jackson index to quantify the relationship between geology, landscape structure, and water transit time in steep wet headwaters. *Hydrological Processes*, *34*, 2139–2150.

Garvelmann, J., Warscher, M., Leonhardt, G., Franz, H., Lotz, A., & Kunstmann, H. (2017). Quantification and characterization of the dynamics of spring and stream water systems in the Berchtesgaden Alps with a long-term stable isotope dataset. *Environmental Earth Sciences*, *76*(22). http://doi.org/10.1007/s12665-017-7107-6

Godsey, S. E., Aas, W., Clair, T. A., de Wit, H. A., Fernandez, I. J., Kahl, J. S., Malcolm, I. A., Neal, C., Neal, M., Nelson, S. J., Norton, S. A., Palucis, M. C., Skjelkvåle, B. L., Soulsby, C., Tetzlaff, D., & Kirchner, J. W. (2010). Generality of fractal 1/f scaling in catchment tracer time series, and its implications for catchment travel time distributions. *Hydrological Processes*, *24*(12), 1660–1671. http://doi.org/10.1002/hyp.7677

Gómez-Gener, L., Lupon, A., Laudon, H., & Sponseller, R. A. (2020). Drought alters the biogeochemistry of boreal stream networks. *Nature Communications*, *11*, 1795.

Groning, M., Lutz, H. O., Roller-Lutz, Z., Kralik, M., Gourcy, L., & Poltenstein, L. (2012). A simple rain collector preventing water re-evaporation dedicated for delta O-18 and delta H-2 analysis of cumulative precipitation samples. *Journal of Hydrology*, *448*, 195–200.

Hale, V. C., & McDonnell, J. J. (2016). Effect of bedrock permeability on stream base flow mean transit time scaling relations: 1. A multiscale catchment intercomparison. *Water Resources Research*, *52*, 1358–1374.

Harman, C. J. (2015). Time-variable transit time distributions and transport: Theory and application to storage-dependent transport of chloride in a watershed. *Water Resources Research*, *51*, 1–30.

Harr, R. D., & McCorison, F. M. (1979). Initial effects of clearcut logging on size and timing of peak flows in a small watershed in western Oregon. *Water Resources Research*, *15*, 90–94.

Heidbuchel, I., Troch, P. A., & Lyon, S. W. (2013). Separating physical and meteorological controls of variable transit times in zero-order catchments. *Water Resources Research*, *49*, 7644–7657.

Heidbuechel, I., Troch, P. A., Lyon, S. W., & Weiler, M. (2012). The master transit time distribution of variable flow systems. *Water Resources Research*, *48*, W06520. https://doi.org/10.1029/2011WR011293

Hrachowitz, M., Fovet, O., Ruiz, L., & Savenije, H. H. G. (2015). Transit time distributions, legacy contamination and variability in biogeochemical $1/f^{\alpha}$ scaling: How are hydrological response dynamics linked to water quality at the catchment scale? *Hydrological Processes*, *29*, 5241–5256.

Hrachowitz, M., Soulsby, C., Tetzlaff, D., Dawson, J. J. C., Dunn, S. M., & Malcolm, I. A. (2009). Using long-term data sets to understand transit times in contrasting headwater catchments. *Journal of Hydrology*, *367*, 237–248.

Hrachowitz, M., Soulsby, C., Tetzlaff, D., Dawson, J. J. C., & Malcolm, I. A. (2009). Regionalization of transit time estimates in montane catchments by integrating landscape controls. *Water Resources Research*, *45*, W05421. https://doi.org/10.1029/2008WR007496

Hrachowitz, M., Soulsby, C., Tetzlaff, D., & Malcolm, I. A. (2011). Sensitivity of mean transit time estimates to model conditioning and data availability. *Hydrological Processes*, *25*, 980–990.

Hrachowitz, M., Soulsby, C., Tetzlaff, D., Malcolm, I. A., & Schoups, G. (2010). Gamma distribution models for transit time estimation in catchments: Physical interpretation of parameters and implications for time-variant transit time assessment. *Water Resources Research*, *46* (10), W10536. http://doi.org/10.1029/2010wr009148

Jasechko, S., Kirchner, J. W., Welker, J. M., & McDonnell, J. J. (2016). Substantial proportion of global streamflow less than three months old. *Nature Geoscience*, *9*, 126–129.

Johnson, S., Wondzell, S., & Rothacher, J. (2019). In L.-T. E. Research (Ed.), *Stream Discharge in Gaged Watersheds at the HJ Andrews Experimental Forest, 1949 to Present*. Forest Science Data Bank.

Jutebring Sterte, E., Lidman, F., Lindborg, E., Sjöberg, Y., & Laudon, H. (2021). How catchment characteristics influence hydrological pathways and travel times in a boreal landscape. *Hydrology and Earth System Sciences*, *25*, 2133–2158.

Kirchner, J. (2016a). Aggregation in environmental systems – Part 1: Seasonal tracer cycles quantify young water fractions, but not mean transit times, in spatially heterogeneous catchments. *Hydrology and Earth System Sciences*, *20*, 279–297.

Kirchner, J. W. (2016b). Aggregation in environmental systems – Part 2: Catchment mean transit times and young water fractions under hydrologic nonstationarity. *Hydrology and Earth System Sciences*, *20*, 299–328.

Kirchner, J. W., Feng, X., & Neal, C. (2000). Fractal stream chemistry and its implications for contaminant transport in catchments. *Nature*, *403*, 524–527.

Kleine, L., Tetzlaff, D., Smith, A., Wang, H. L., & Soulsby, C. (2020). Using water stable isotopes to understand evaporation, moisture stress, and re-wetting in catchment forest and grassland soils of the summer drought of 2018. *Hydrology and Earth System Sciences*, *24*, 3737–3752.

Lane, D., McCarter, C. P. R., Richardson, M., McConnell, C., Field, T., Yao, H., Arhonditsis, G., & Mitchell, C. P. J. (2020). Wetlands and low-gradient topography are associated with longer hydrologic transit times in precambrian shield headwater catchments. *Hydrological Processes*, *34*, 598–614.

Laudon, H., & Sponseller, R. A. (2017). How landscape organization and scale shape catchment hydrology and biogeochemistry: Insights from a long-term catchment study. *Wiley Interdisciplinary Reviews: Water*, *5*, 265.

Leach, J. A., Buttle, J. M., Webster, K. L., Hazlett, P. W., & Jeffries, D. S. (2020). Travel times for snowmelt-dominated headwater catchments: Influences of wetlands and forest harvesting, and linkages to stream water quality. *Hydrological Processes*, *34*, 2154–2175.

Liu, Z., Yoshmura, K., Bowen, G. J., & Welker, J. M. (2014). Pacific–North American Teleconnection controls on precipitation isotopes (δ18O) across the contiguous United States and adjacent regions: A GCM-based analysis. *Journal of Climate*, *27*, 1046–1061.

Lowe, W., & Likens, G. (2005). Moving headwater streams to the head of the class. *Bioscience*, *55*, 196–197.

Lutz, S. R., Krieg, R., Müller, C., Zink, M., Knöller, K., Samaniego, L., & Merz, R. (2018). Spatial patterns of water age: Using young water fractions to improve the characterization of transit times in contrasting catchments. *Water Resources Research*, *54*, 4767–4784.

Małoszewski, P., & Zuber, A. (1982). Determining the turnover time of groundwater systems with the aid of environmental tracers. *Journal of Hydrology*, *57*, 207–231.

McGill, L. M., Brooks, J. R., & Steel, E. A. (2021). Spatiotemporal dynamics of water sources in a mountain river basin inferred through δ2H and δ18O of water. *Hydrological Processes*, *35*, e14063.

McGlynn, B., McDonnell, J., Stewart, M., & Seibert, J. (2003). On the relationships between catchment scale and streamwater mean residence time. *Hydrological Processes*, *17*, 175–181.

McGuire, K. J., DeWalle, D. R., & Gburek, W. J. (2002). Evaluation of mean residence time in subsurface waters using oxygen-18 fluctuations during drought conditions in the mid-Appalachians. *Journal of Hydrology*, *261*, 132–149.

McGuire, K. J., & McDonnell, J. J. (2006). A review and evaluation of catchment transit time modeling. *Journal of Hydrology*, *330*, 543–563.

McGuire, K. J., McDonnell, J. J., Weiler, M., Kendall, C., McGlynn, B. L., Welker, J. M., & Seibert, J. (2005). The role of topography on catchment-scale water residence time. *Water Resources Research*, *41*, 5002.

Mosquera, G. M., Segura, C., Vache, K. B., Windhorst, D., Breuer, L., & Crespo, P. (2016). Insights into the water mean transit time in a high-elevation tropical ecosystem. *Hydrology and Earth System Sciences*, *20*, 2987–3004.

Mote, P. W., Hamlet, A. F., Clark, M. P., & Lettenmaier, D. P. (2005). Declining mountain snowpack in western North America. *Bulletin of the American Meteorological Society*, *86*, 39.

Mote, P. W., Li, S., Lettenmaier, D. P., Xiao, M., & Engel, R. (2018). Dramatic declines in snowpack in the western US. NPJ climate and atmospheric. *Science*, *1*, 2.

Mueller, M. H., Weingartner, R., & Alewell, C. (2013). Importance of vegetation, topography and flow paths for water transit times of base flow in alpine headwater catchments. *Hydrology and Earth System Sciences*, *17*, 1661–1679.

Muñoz-Villers, L. E., Geissert, D. R., Holwerda, F., & Mcdonnell, J. J. (2016). Factors influencing stream baseflow transit times in tropical montane watersheds. *Hydrology and Earth System Sciences*, *20*, 1621–1635.

Mwakalila, S., Feyen, J., & Wyseure, G. (2002). The influence of physical catchment properties on baseflow in semi-arid environments. *Journal of Arid Environments*, *52*, 245–258.

Nusbaumer, J., & Noone, D. (2018). Numerical evaluation of the modern and future origins of atmospheric river moisture over the west coast of the United States. *Journal of Geophysical Research: Atmospheres*, *123*, 6423–6442.

Nusbaumer, J., Wong, T. E., Bardeen, C., & Noone, D. (2017). Evaluating hydrological processes in the community atmosphere model version 5 (CAM5) using stable isotope ratios of water. *Journal of Advances in Modeling Earth Systems*, *9*, 949–977.

Peralta-Tapia, A., Soulsby, C., Tetzlaff, D., Sponseller, R., Bishop, K., & Laudon, H. (2016). Hydroclimatic influences on non-stationary transit time distributions in a boreal headwater catchment. *Journal of Hydrology*, *543*, 7–16.

Perkins, R. M., & Jones, J. A. (2008). Climate variability, snow, and physiographic controls on storm hydrographs in small forested basins, western cascades, Oregon. *Hydrological Processes*, *22*, 4949–4964.

Price, K. (2011). Effects of watershed topography, soils, land use, and climate on baseflow hydrology in humid regions: A review. *Progress in Physical Geography*, *35*, 465–492.

Rodgers, P., Soulsby, C., Waldron, S., & Tetzlaff, D. (2005). Using stable isotope tracers to assess hydrological flow paths, residence times and landscape influences in a nested mesoscale catchment. *Hydrology and Earth System Sciences*, *9*, 139–155.

Schmieder, J., Seeger, S., Weiler, M., & Strasser, U. (2019). "Teflon Basin" or not? A high-elevation catchment transit time modeling approach. *Hydrology*, *6*, 92.

Sebestyen, S. D., Shanley, J. B., Boyer, E. W., Kendall, C., & Doctor, D. H. (2014). Coupled hydrological and biogeochemical processes controlling variability of nitrogen species in streamflow during autumn in an upland forest. *Water Resources Research*, *50*, 1569–1591.

Seeger, S., & Weiler, M. (2014). Reevaluation of transit time distributions, mean transit times and their relation to catchment topography. *Hydrology and Earth System Sciences*, *18*, 4751–4771.

Segura, C. (2019). In L.-T. E. Research (Ed.), *Water Stable Isotopes for Streams and Precipitation Samples in the HJ Andrews Experimental Forest and Mary's River Watershed, 2014-2016*. Forest Science Data Bank.

Segura, C., Noone, D., Warren, D., Jones, J. A., Tenny, J., & Ganio, L. (2019). Climate, landforms, and geology affect baseflow sources in a mountain catchment. *Water Resources Research*, *55*, 5238–5254.

Simon, R., Klaudija, S., Metka, P., Sonja, L., & Nejc, B. (2019). Identifying the hydrological behavior of a complex karst system using stable isotopes. *Journal of Hydrology*, *577*, 123956.

Smith, M. W. (2014). Roughness in the earth sciences. *Earth-Science Reviews*, *136*, 202–225.

Soulsby, C., & Tetzlaff, D. (2008). Towards simple approaches for mean residence time estimation in ungauged basins using tracers and soil distributions. *Journal of Hydrology*, *363*, 60–74.

Soulsby, C., Tetzlaff, D., Rodgers, P., Dunn, S., & Waldron, S. (2006). Runoff processes, stream water residence times and controlling landscape characteristics in a mesoscale catchment: An initial evaluation. *Journal of Hydrology*, *325*, 197–221.

Spies, T. (2016). In L.-T. E. Research (Ed.), *LiDAR Data (August 2008) for the Andrews Experimental Forest and Willamette National Forest Study Areas*. Forest Science Data Bank.

Stewart, M. K., Morgenstern, U., & McDonnell, J. J. (2010). Truncation of stream residence time: How the use of stable isotopes has skewed our concept of streamwater age and origin. *Hydrological Processes*, *24*, 1646–1659.

Stockinger, M. P., Bogena, H. R., Lücke, A., Stumpp, C., & Vereecken, H. (2019). Time variability and uncertainty in the fraction of young water in a small headwater catchment. *Hydrology and Earth System Sciences*, *23*, 4333–4347.

Swanson, F., & James, M. (1975). Geology and geomorphology of the H.J. Andrews Experimental Forest, western Cascades, Oregon (PNW-188). U.S. Department of Agriculture, Forest Service, Pacific Northwest Forest and Range Experiment Station: Portland, OR, 14.

Swanson, F. J., & Jones, J. A. (2002). Geomorphology and hydrology of the HJ Andrews experimental forest, Blue River, Oregon. *Field Guide to Geologic Processes in Cascadia*, *1*, 289–313.

Tague, C., & Grant, G. E. (2004). A geological framework for interpreting the low-flow regimes of cascade streams, Willamette River basin, Oregon. *Water Resources Research*, *40*, 4303.

Tague, C. L., Choate, J. S., & Grant, G. (2013). Parameterizing sub-surface drainage with geology to improve modeling streamflow responses to climate in data limited environments. *Hydrology and Earth System Sciences*, *17*, 341–354.

Tetzlaff, D., Malcolm, I., & Soulsby, C. (2007). Influence of forestry, environmental change and climatic variability on the hydrology, hydrochemistry and residence times of upland catchments. *Journal of Hydrology*, *346*, 93–111.

Tetzlaff, D., Seibert, J., McGuire, K. J., Laudon, H., Burns, D. A., Dunn, S. M., & Soulsby, C. (2009). How does landscape structure influence catchment transit time across different geomorphic provinces? *Hydrological Processes*, *23*, 945–953.

Timbe, E., Windhorst, D., Crespo, P., Frede, H.-G., Feyen, J., & Breuer, L. (2014). Understanding uncertainties when inferring mean transit times of water trough tracer-based lumped-parameter models in Andean tropical montane cloud forest catchments. *Hydrology and Earth System Sciences*, *18*, 1503–1523.

Trinh, A. D., Do, T. N., Panizzo, V. N., McGowan, S., & Leng, M. J. (2020). Using stable isotopes to estimate young water fractions in a heavily regulated, tropical lowland river basin. *Hydrological Processes*, *34*, 4239–4250.

Vano, J. A., Nijssen, B., & Lettenmaier, D. P. (2015). Seasonal hydrologic responses to climate change in the Pacific northwest. *Water Resources Research*, *51*, 1959–1976.

Verfaillie, D., Lafaysse, M., Déqué, M., Eckert, N., Lejeune, Y., & Morin, S. (2018). Multi-component ensembles of future meteorological and natural snow conditions for 1500 m altitude in the chartreuse mountain range, northern French Alps. *The Cryosphere*, *12*, 1249–1271.

von Freyberg, J., Allen, S. T., Seeger, S., Weiler, M., & Kirchner, J. W. (2018). Sensitivity of young water fractions to hydro-climatic forcing and landscape properties across 22 Swiss catchments. *Hydrology and Earth System Sciences*, *22*, 3841–3861.

Warix, S. R., Godsey, S. E., Lohse, K. A., & Hale, R. L. (2021). Influence of groundwater and topography on stream drying in semi-arid headwater streams. *Hydrological Processes*, *35*, e14185.

Woods, R., & Rowe, L. (1996). The changing spatial variability of subsurface flow across a hillside. *Journal of Hydrology*, *35*, 51–86.

Wu, J., Yang, Q., & Li, Y. (2018). Partitioning of terrain features based on roughness. *Remote Sensing*, *10*, 1985.

Wymore, A. S., Brereton, R. L., Ibarra, D. E., Maher, K., & McDowell, W. H. (2017). Critical zone structure controls concentration-discharge relationships and solute generation in forested tropical montane watersheds. *Water Resources Research.*, *53*, 6279–6295.

Zhang, Q., Knowles, J. F., Barnes, R. T., Cowie, R. M., Rock, N., & Williams, M. W. (2018). Surface and subsurface water contributions to streamflow from a mesoscale watershed in complex mountain terrain. *Hydrological Processes*, *32*, 954–967.

Zhang, Z., Chen, X., Cheng, Q., & Soulsby, C. (2020). Characterizing the variability of transit time distributions and young water fractions in karst catchments using flux tracking. *Hydrological Processes*, *34*, 3156–3174.

SUPPORTING INFORMATION

Additional supporting information may be found in the online version of the article at the publisher's website.

How to cite this article: Segura, C. (2021). Snow drought reduces water transit times in headwater streams. *Hydrological Processes*, *35*(12), e14437. https://doi.org/10.1002/hyp.14437